ChemPubSoc Europe

DOI: 10.1002/chem.201903498

CHEMISTRY A European Journal Full Paper

Anion Encapsulation

A Tris(3-pyridyl)stannane as a Building Block for Heterobimetallic Coordination Polymers and Supramolecular Cages

Eric S. Yang,[a] Alex J. Plajer,[a] Álvaro García-Romero,[b] Andrew D. Bond,[a] Tanya K. Ronson,[a] Celedonio M. Álvarez,[b] Raúl García-Rodríguez,*[b] Annie L. Colebatch,*[a, c] and Dominic S. Wright*[a]

Abstract: The systematic assembly of supramolecular arrangements is a persistent challenge in modern coordination chemistry, especially where further aspects of complexity are concerned, as in the case of large molecular mixed-metal arrangements. One targeted approach to such heterometallic complexes is to engineer metal-based donor ligands of the correct geometry to build 3D arrangements upon coordination to other metals. This simple idea has, however, only rarely been applied to main group metal-based ligand systems. Here, we show that the new, bench-stable tris(3-pyridyl)stannane ligand $PhSn(3\text{-}Py)_3$ (3-Py = 3-pyridyl) provides simple access to a range of heterometallic Sn^{IV}/transition metal complexes, and that the presence of weakly coordinating counter anions can be used to build discrete molecular arrangements involving anion encapsulation. This work therefore provides a building strategy in this area, which parallels that of supramolecular transition metal chemistry.

Introduction

Pyridyl substituents are one of the most commonly encountered donor groups in coordination chemistry. However, while ligand assemblies containing 2-pyridyl-based ligands are pervasive in coordination chemistry, and counterparts containing 4-pyridyl-derived groups have been widely used in supramolecular self-assembly,[1] their 3-pyridyl relatives have thus far been underutilised. Like 4-pyridyl linkers, 3-pyridyl substituents can act as metal-bridging ligands but give rise to different supramolecular architectures as a direct result of the different disposition of the *N*-donor atoms within the ligand nodes. The comparative absence of ligands based on 3-pyridyl donor sets has been ascribed to inherent synthetic difficulties[1] and also to their conformational flexibility, which entropically favours formation of small aggregates.[2] Severin and co-workers have overcome this tendency by incorporating additional steric groups into bis(3-pyridyl) Fe clathrochelate ligands to produce $Pd_6L_{12}{}^{12+}$ cages,[2] and have found that tuning the sterics alters the size of the cage.[3] This metalloligand strategy for the construction of heterometallic supramolecular architectures has been successfully enacted for a variety of mixed transition metal systems, for example, Fe/Pd,[2,4–6] Fe/Ru,[7] Fe/Co,[8,9] Co/Mn[5] and Ru/Pd.[10,11] However, the use of main group metalloligands to create mixed main group/transition metal heterometallic systems is rare.

We have developed a family of tris(2-pyridyl) ligands featuring main group bridgeheads $E(2\text{-}Py)_3$ (Figure 1 a)[12–15] and demonstrated that the nature of the bridgehead atom can be used to modulate structure and reactivity.[16] However, the corresponding tris(3-pyridyl) ligands, especially those featuring main group bridgehead atoms (limited to Si, P and Bi), have seen only limited use in the literature. Notably, Reek has employed $P(3\text{-}Py)_3$ as a ligand template to construct well-defined catalytic cavities for regioselective hydroformylation.[17,18] Boomishankar has also used the silyl ligand $MeSi(3\text{-}Py)_3$ and its 3-quinolyl analogue $MeSi(3\text{-}Qy)_3$ to obtain a series of 2D metal-organic frameworks (MOFs)[19] and one example of a discrete molecular cage (e.g., Figure 1 b).[20] It can be noted, however, that although obtained in high yields these previously investigated P- and MeSi-bridgehead tris(3-pyridyl) ligands are either air sensitive and/or require chromatographic purification, making them time-consuming or difficult to prepare and handle.[19,21]

As part of our continued development of main group tris(pyridyl) coordination chemistry, in this paper we utilise the readily-prepared, bench-stable tris(3-pyridyl)stannane ligand

[a] *E. S. Yang, A. J. Plajer, Dr. A. D. Bond, Dr. T. K. Ronson, Dr. A. L. Colebatch, Prof. D. S. Wright*
Department of Chemistry, University of Cambridge
Lensfield Road
Cambridge, CB2 1EW (UK)
E-mail: dsw1000@cam.ac.uk

[b] *Á. García-Romero, C. M. Álvarez, Dr. R. García-Rodríguez*
GIR MIOMeT-IU Cinquima-Química Inorgánica Facultad de Ciencias
Universidad de Valladolid
Campus Miguel, Delibes
47011 Valladolid (Spain)
E-mail: raul.garcia.rodriguez@uva.es

[c] *Dr. A. L. Colebatch*
Research School of Chemistry
Australian National University
Canberra, ACT, 2601 (Australia)
E-mail: annie.colebatch@anu.edu.au

Supporting information and the ORCID identification number(s) for the author(s) of this article can be found under: https://doi.org/10.1002/chem.201903498.

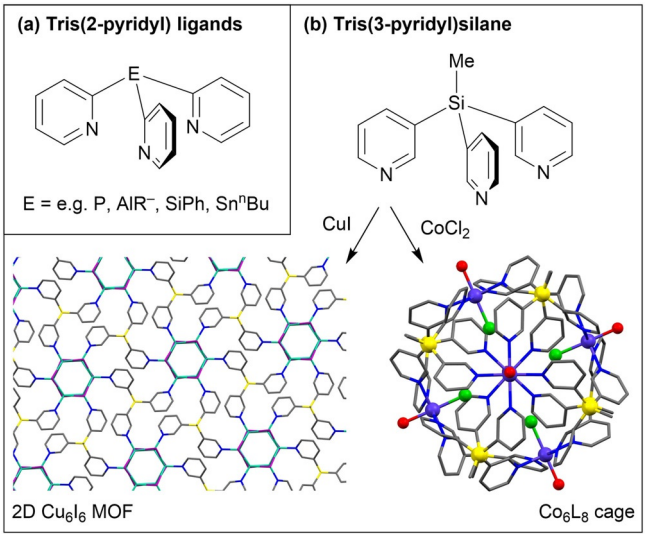

Figure 1. a) Structure of tris(2-pyridyl) ligands containing a selection of bridgehead atoms. b) Previous studies by Boomishankar and co-workers involving the $MeSi(3\text{-}Py)_3$ ligand in which polymeric structures or discrete molecular cages were obtained, depending on the conditions and/or the transition metal coordinated.[19,20]

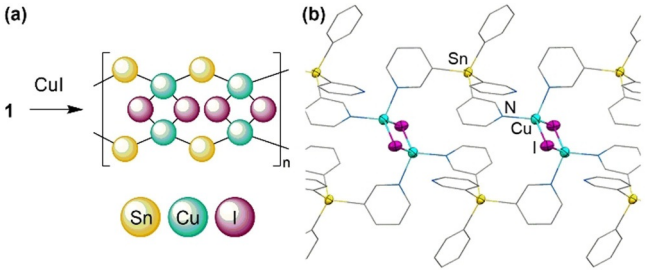

Figure 3. a) Synthesis of $[Cu_2I_2(\mathbf{1})_2]_n$. b) X-ray crystal structure of $[Cu_2I_2(\mathbf{1})_2]_n$. Displacement ellipsoids are drawn at 50% probability, hydrogen atoms are omitted. Selected bond lengths (Å) and angles (°): Cu1—N1 2.015(12), Cu1—N2 2.086(12), Cu1—I1 2.694(3)/2.577(2); N1-Cu1-N2 108.7(5), N2-Cu1-I1 99.1(3)/105.7(4).

$PhSn(3\text{-}Py)_3$, which provides straightforward access to a range of new heterobimetallic supramolecular arrangements. We show that the architectures of complexes formed with transition metals can be strongly influenced by the nature of the bridgehead group and the presence of weakly-coordinating anions (which can promote the formation of discrete cages that involve anion encapsulation).

Results and Discussion

The ligand $PhSn(3\text{-}Py)_3$ (**1**) was obtained in the one-pot reaction of 3-BrPy with the turbo-Grignard *i*PrMgCl·LiCl at −15 °C,[22] followed by addition of $PhSnCl_3$ (Figure 2a, see Experimental Section). Compound **1** is seemingly indefinitely air- and moisture-stable and is readily isolated as colourless crystals in 36% yield after crystallisation from dichloromethane/hexane, without the need for column chromatography. In addition to analytical and spectroscopic data (see Experimental Section), the single-crystal X-ray structure (Figure 2b) does not show Mg^{2+} coordination to **1** in its synthesis, as can commonly

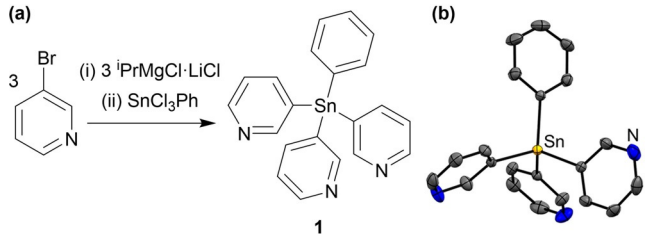

Figure 2. a) Synthesis of $PhSn(3\text{-}Py)_3$ (**1**). b) X-ray crystal structure of **1**. Thermal ellipsoids are drawn at 50% probability, hydrogen atoms are omitted. Selected bond lengths (Å) and angles (°): Sn1—C1 2.139(4); C1-Sn1-C1^{i} 109.17(11), Sn1-C1-C2 120.9(3).

occur in this area.[7,16] This is important because the presence of a contaminant metal ion can be a complication in ligand transfer to other metals.

Slow diffusion of an MeCN solution of **1** (1 equiv) into an MeCN solution of CuI (1 equiv) over three days in air gave yellow crystals of $[Cu_2I_2(\mathbf{1})_2]_n$ in 66% yield (Figure 3) (see Experimental Section). The X-ray crystal structure is that of a 1D coordination polymer in which bridging ligands **1** link Cu_2I_2 units in a polymeric arrangement, using two of the three 3-Py N donor atoms (with the third being uncoordinated). This arrangement is very similar to that of $[Cu_2I_2\{MeSi(3\text{-}Qy)_3\}_2]_n$ obtained using the tris(3-quinolyl) ligand.[19] However, it is interesting to note that the more closely related $MeSi(3\text{-}Py)_3$ ligand does not form this structure with CuI, instead producing a 2D $[Cu_6I_6]$-cluster MOF.[11] Attempts to produce a similar arrangement to the latter using the same solvothermal conditions as in the previous study only produced intractable mixtures of products, regardless of stoichiometry. Thus it appeared from this initial study that simply changing the bridgehead group from $MeSi(3\text{-}Py)_3$ to $PhSn(3\text{-}Py)_3$ leads to marked differences in coordination character.[16] This can be ascribed to two factors: (i) the change in ligand bite resulting from the incorporation of a larger atom at the bridging position and (ii) potentially also to the differing steric influence of the Ph-group of **1** compared to the Me-group of $MeSi(3\text{-}Py)_3$.

A radically different outcome is observed in the coordination of **1** to $CuPF_6$, containing a weakly-coordinating anion. The 1:1 reaction of **1** with $[Cu(NCMe)_4]PF_6$ gives the complex $[Cu(\mathbf{1})(NCMe)]_4[PF_6]_4$ in 91% isolated yield (Figure 4) (see Experimental Section). The X-ray crystal structure shows a cage arrangement in which four of the ligands **1** bridge the four Cu centres, using all three pyridyl arms, into a discrete $[\{Cu(\mathbf{1})(NCMe)\}_4(\subset PF_6)]^{3+}$ cation. The Cu^{I} ions are also each coordinated by an MeCN molecule, resulting in a distorted tetrahedral metal geometry. One of the PF_6^- ions is encapsulated at the centre of the $[\{Cu(\mathbf{1})(NCMe)\}_4(\subset PF_6)]^{3+}$ cation, while the remaining three anions are located in the crystal lattice. The nearest (3-Py)C···F contacts to the encapsulated PF_6^- anion (3.17(1)–3.67(1) Å) are all at or above the sum of the van der Waals radii of F and C (3.17 Å),[23] with the Py rings tilted away

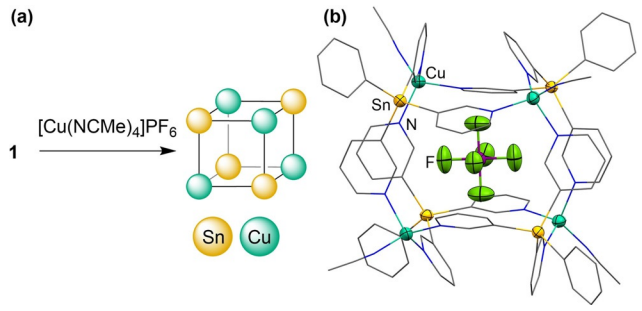

Figure 4. a) Synthesis of the cage $[Cu(\mathbf{1})(NCMe)]_4[PF_6]_4$. b) X-ray crystal structure of $[Cu(\mathbf{1})(NCMe)]_4[PF_6]_4$. Displacement ellipsoids are drawn at 50% probability, hydrogen atoms and *exo*-PF_6^- ions are omitted. Selected bond lengths (Å) and angles (°): Cu1–N1 2.026(7), Cu1–N7 1.951(9); N1-Cu1-N5 107.9(3), N1-Cu1-N7 122.9(3), C4-Sn1-C39 108.5(3).

from the centroid of the cage in order to accommodate the PF_6^- anion in the cavity.

^1H and ^{19}F NMR spectroscopic studies of $[\{Cu(\mathbf{1})(NCMe)\}_4(\subset PF_6)]^{3+}$ in CD_3CN indicate dynamic behaviour. At 298 K the ^1H NMR spectrum consists of broad signals that have similar chemical shifts to those observed for the free ligand **1**, together with a set of lower intensity signals (see the Supporting Information, Figure S5). As the temperature is decreased the latter signals increase in intensity and are practically the only species observed at 228 K. While the ^{19}F NMR spectrum above 298 K indicates only one (averaged) PF_6^- environment, at 228 K two major PF_6^- environments are found at $\delta = -72.4$ (3F, $^1J_{P\text{-}F} = 706$ Hz) and -71.0 (1F, $^1J_{P\text{-}F} = 717$ Hz) ppm, together with a further (minor) PF_6^- environment at $\delta = -70.9$ ppm (Figure 5). The ^{19}F and ^1H NMR spectra are also concentration-dependent, with the low-temperature species being favoured in more concentrated samples and the high-temperature species being favoured in dilute solutions (Figure S7 in the Supporting Information). The concentration- and temperature-dependence of the ^1H and ^{19}F NMR spectra are consistent with a dynamic process involving dissociation of the cage $[Cu(\mathbf{1})(NCMe)]_4[PF_6]_4$ into smaller species at higher temperatures and lower concentrations. Variable-temperature NMR experiments also confirm that the observed equilibrium is completely reversible. On the basis of the integration of the ^{19}F NMR signals at 228 K, we assign the resonance at $\delta = -71.0$ to the cage-encapsulated PF_6^- environment of the $[\{Cu(\mathbf{1})(NCMe)\}_4(\subset PF_6)]^{3+}$ cation and the resonance at $\delta = -72.4$ ppm to the free PF_6^- counter-anions (found in the expected 1:3 ratio, respectively).

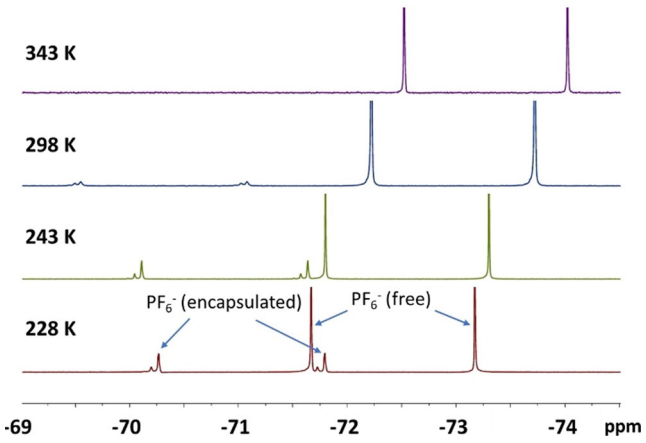

Figure 5. ^{19}F NMR spectra of $[Cu(\mathbf{1})(NCMe)]_4[PF_6]_4$ at 343, 298, 243 and 228 K.

Further support for the previous conclusion comes from ^1H and ^{19}F DOSY NMR experiments (Figure 6). ^{19}F DOSY NMR experiments at 228 K show two markedly different diffusion coefficients for the doublet resonances at $\delta = -72.4$ (3F, 6.19×10^{-10} $m^2 s^{-1}$) and -71.0 (1F, 2.06×10^{-10} $m^2 s^{-1}$). The diffusion coefficient extracted from ^1H DOSY (2.16×10^{-10} $m^2 s^{-1}$) is identical to that for the ^{19}F NMR resonance at $\delta = -71.0$ ppm at this temperature (Figure 6), supporting the conclusion that this resonance corresponds to the encapsulated PF_6^- anion of the intact $[\{Cu(\mathbf{1})(NCMe)\}_4(\subset PF_6)]^{3+}$ cation, while the free PF_6^- counterions at $\delta = -72.4$ ppm diffuse much faster. The minor ^{19}F resonance at $\delta = -70.9$ ppm has a very similar diffusion coefficient to the encapsulated PF_6^- anion, suggesting that this

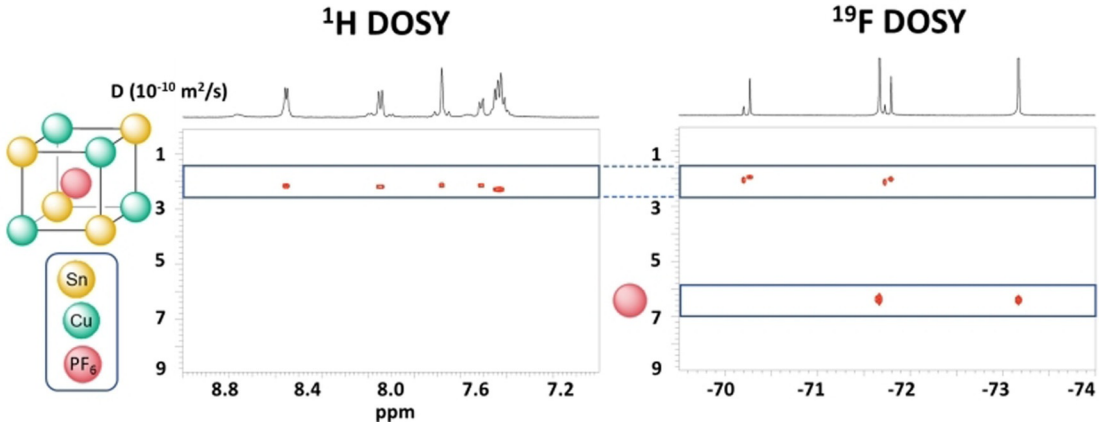

Figure 6. ^1H DOSY (left) and ^{19}F DOSY (right) of $[Cu(\mathbf{1})(NCMe)]_4[PF_6]_4$ in CD_3CN at 228 K. The ^{19}F DOSY spectrum shows that the encapsulated PF_6^- ion diffuses with the same diffusion coefficient (2.06×10^{-10} $m^2 s^{-1}$) as that observed in the ^1H DOSY spectrum (2.16×10^{-10} $m^2 s^{-1}$) for the intact cage, whereas the free PF_6^- counterions diffuse much faster.

arises from an encapsulated PF_6^- anion within a cage closely related to the $[Cu(\mathbf{1})(NCMe)]_4^{4+}$ cation.

In contrast, the 1:1 reaction of **1** with $AgPF_6$ in MeCN does not result in the formation of a discrete molecular structure. While the ligands **1** adopt a similar coordination mode to that in $[Cu(\mathbf{1})(NCMe)]_4[PF_6]_4$, involving all three of the pyridyl-N atoms, the product $\{[Ag(\mathbf{1})(NCMe)]PF_6{\cdot}OEt_2\}_n$ is a 2D-coordination polymer (Figure 7) (see Experimental Section). The network is composed of fused Ag_3Sn_3 rings, with the PF_6^- anions interspersed within the 2D network, and forming weak F···Ag interactions with some of the Ag^+ cations (less than the sum of the van der Waals radii). The presence of these F···Ag interactions is not surprising bearing in mind the larger ionic radius and more electropositive character of Ag^+, and provides a potential reason why a polymeric structure is formed in this case rather than a discrete cage (cf. no such interactions in $[Cu(\mathbf{1})(NCMe)]_4[PF_6]_4$). Variable-temperature ^1H and ^{19}F NMR spectroscopic studies in MeCN show that a single species is present in solution, which does not involve PF_6^- encapsulation (Supporting Information, Figures S11–S15).

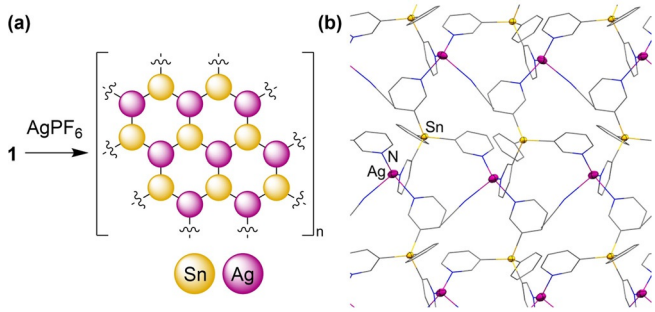

Figure 7. a) Synthesis of $\{[Ag(\mathbf{1})(NCMe)]PF_6{\cdot}OEt_2)_n$. b) X-ray crystal structure of the 2D sheet $\{[Ag(\mathbf{1})(NCMe)]PF_6{\cdot}OEt_2\}_n$. Displacement ellipsoids are drawn at 50% probability. Hydrogen atoms, PF_6^- ions and Et_2O solvent molecules in the lattice are omitted. Selected bond lengths (Å): Ag–N range 2.219(4)–2.628(6).

Attempts to extend this work to Au^I by reaction of **1** with AuCl(THT) (THT = tetrahydrothiophene) resulted in reduction to Au^0. However, coordination of **1** to other transition metals was more successful. Cobalt(II) was selected as a promising candidate as Boomishankar has reported preparation of a $[Co_6Cl_6\{MeSi(3\text{-}Py)_3\}_8(H_2O)_6]Cl_3$ cage using the same salt, $CoCl_2$.[20] The 1:1 reaction of **1** with $CoCl_2$ in MeOH yielded a pink solution from which a blue solid was obtained by slow solvent evaporation. Recrystallisation from MeOH/Et_2O yielded $[CoCl_2(\mathbf{1})(MeOH)]_n$ as pink crystals (in 47% yield) suitable for (synchrotron) X-ray crystallography (Figure 8) (see Experimental Section). The MeOH ligands that are coordinated to the Co^{2+} in the complex are highly labile and are rapidly lost when the solid complex is isolated, giving the blue solid that was originally observed. The colour change from pink to blue is consistent with a change in coordination geometry from octahedral to tetrahedral. Characterisation of $[CoCl_2(\mathbf{1})(MeOH)]_n$ by ^1H NMR spectroscopy was not possible due to the paramagnetism of Co^{II}.

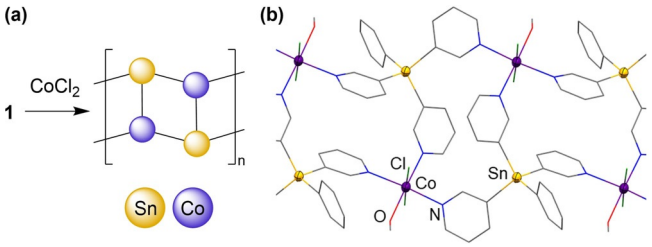

Figure 8. a) Synthesis of $[CoCl_2(\mathbf{1})(MeOH)]_n$. b) X-ray crystal structure of $[CoCl_2(\mathbf{1})(MeOH)]_n$. Displacement ellipsoids are drawn at 50% probability. Hydrogen atoms are omitted. Selected bond lengths (Å) and angles (°): Co1–N1 2.151(3), Co1–O1 2.130(2), Co1–Cl1 2.4495(9), Co1–Cl2 2.4574(9); N1-Co1-N2 91.76(10), N2-Co1-N3 175.79(10).

The solid-state structure of $[CoCl_2(\mathbf{1})(MeOH)]_n$ is that of a 1D coordination polymer composed of fused Co_2Sn_2 rings, in which the three 3-Py arms of each of the ligands **1** bridge the Co^{II} centres. The formation of this coordination polymer is distinctly different from the $[Co_6Cl_6\{MeSi(3\text{-}Py)_3\}_8(H_2O)_6]^{3+}$ cage arrangement obtained using the analogous silicon ligand $MeSi(3\text{-}Py)_3$ with $CoCl_2$ (Figure 1b),[20] again suggesting the importance of the steric and geometric profile of the bridgehead group of the tris(pyridyl) ligand in architectural control.

The influence of a weakly-coordinating anion on the structure of the product was investigated using $Co(BF_4)_2{\cdot}6H_2O$ in place of $CoCl_2$ (Figure 9a). Slow diffusion of a layered MeCN solution of $Co(BF_4)_2{\cdot}6H_2O$ into a CH_2Cl_2 solution of **1** at −30 °C for one week produced pink needles, identified by X-ray crystallography as $[Co_5(\mathbf{1})_6(H_2O)_6(NCMe)_6][BF_4]_{10}$ (in 58% yield) (see Experimental Section) (Figure 9b). The X-ray data show a rapid drop-off in intensity as a function of scattering angle, leading to challenges with the refinement (see ESI), but the connectivity and structural arrangement of the complex are proved unambiguously. The structure was confirmed for several crystals obtained from different reaction batches. The structure contains a cationic $[Co_5(\mathbf{1})_6(H_2O)_6(NCMe)_6(\subset BF_4)_2]^{8+}$ (Co_5Sn_6) cage in which two BF_4^- anions are encapsulated (with the remaining eight residing in the crystal lattice). The five Co^{II} atoms are arranged in a trigonal bipyramid, with each of the six faces of the trigonal bipyramid being face-capped by ligands **1** (which use all three of the 3-Py-N atoms). This trigonal bipyramidal Co_5 core is inscribed within a surrounding Sn_6 triangular prism, maintaining overall approximate C_3 symmetry (Figure 9c). While the axial Co^{II} ions are coordinated by three (3-Py)N atoms, the equatorial Co^{II} ions are coordinated by four (3-Py)N atoms. In addition, these Co^{II} centres are each bonded to an H_2O ligand which is located on the internal surface of the cage and are involved in H···F H-bonding to the encapsulated BF_4^- anions (O···F range 2.74–2.98 Å; cf. sum of van der Waals radii of O and F 2.99 Å).

Although the paramagnetic nature of $[Co_5(\mathbf{1})_6(H_2O)_6(NCMe)_6][BF_4]_{10}$ hampered in-depth ^1H NMR spectroscopic studies, the ^{11}B and ^{19}F NMR spectra in MeCN at room temperature support the retention of the cage structure in solution, with both showing two BF_4^- environments in the expected 1:4 ratio, along with drastically downfield-shifted resonances for the en-

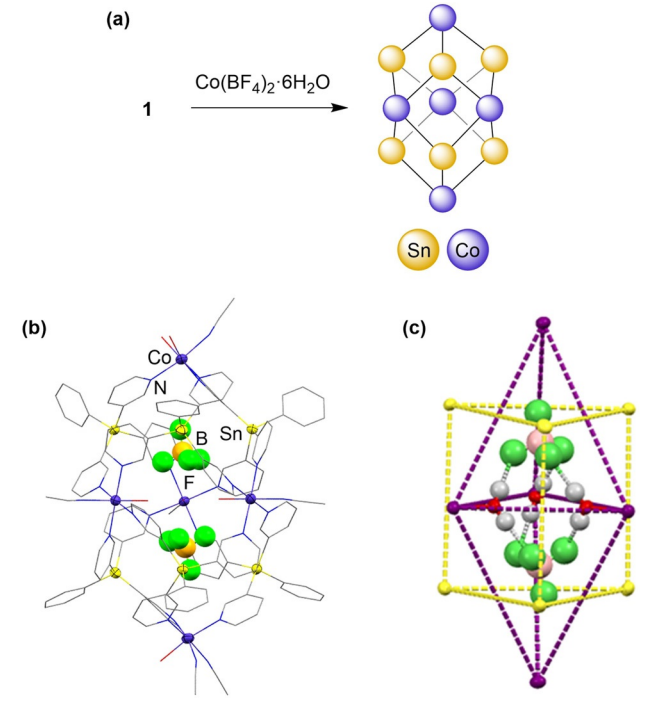

Figure 9. a) Synthesis of $[Co_5(\mathbf{1})_6(H_2O)_6(NCMe)_6][BF_4]_{10}$. b) X-ray crystal structure of the ion $[Co_5(\mathbf{1})_6(H_2O)_6(NCMe)_6)(\subset BF_4)_2]^{8+}$. Displacement ellipsoids are drawn at 50% probability. Hydrogen atoms and *exo*-BF_4^- ions are omitted. Selected bond lengths (Å) and angles (°): Co–N_{py} range 2.105(18)–2.189(17), O···F range 2.74–2.98. c) Connectivity of the metal atoms and the hydrogen bonding within the core, showing the hydrogen bonding of the three internal H_2O molecules to the BF_4^- ions. The complex has approximate C_3 symmetry, with the rotation axis vertical in the diagram.

capsulated BF_4^- anions (e.g., $\delta_F = -112.8$ (1 F), -145.6 ppm (4 F), Supporting Information, Figures S17 and 18).

Conclusion

In conclusion, the PhSn(3-Py)$_3$ ligand **1** is very easily prepared in a one-pot reaction as an air- and water-stable crystalline solid, without the need for purification by column chromatography, and provides a simple building block for the construction of heterobimetallic compounds. Structural studies show that the nature of the coordination compounds formed with **1** is dependent not just on the metal ion coordinated but is also influenced by the coordinating or weakly coordinating nature of the anions. Although weakly coordinating anions are known to encourage the formation of discrete cages in supramolecular transition metal chemistry and crystal engineering in general,[24,25] this effect (as well as anion encapsulation) has not been seen previously in the tris(pyridyl) family of ligands and is a rare example in the area of main group chemistry. Comparison of our results with those involving the closely related MeSi(3-Py)$_3$ ligand indicates that the steric and geometric properties of the bridgehead itself can have a major structure-directing influence. This conclusion should provide large scope for exploring the structural influence of a range of main group bridgeheads in the future, as well as incorporation of reactive or functionalisable main group sites as a new avenue by which to access targeted reactivity in supramolecular constructs.

Experimental Section

Details of general experimental techniques and instrumentation: Syntheses were carried out on a Schlenk line under a nitrogen atmosphere, unless otherwise specified. 3-Bromopyridine was distilled and dried over molecular sieves (4 Å). Other starting materials (e.g., $PhSnCl_3$) were obtained commercially from Sigma–Aldrich and Alfa-Aesar and used as received. MeCN and CH_2Cl_2 were dried over CaH_2 and distilled under nitrogen. Et_2O was dried over Na/benzophenone and distilled under nitrogen. CD_3CN was degassed and dried over molecular sieves (4 Å). Starting materials and products were handled with the aid of a nitrogen-filled glove box (Saffron type α).

Room-temperature ^1H, ^{11}B, and ^{19}F NMR spectra were recorded on a Bruker 400 MHz Avance III HD Smart Probe spectrometer. Variable temperature ^1H and ^{19}F NMR spectra were recorded on a Bruker 500 MHz Avance III HD Smart Probe spectrometer or on a 500 MHz Agilent DD2 spectrometer. 2D ^1H and ^{19}F DOSY spectra were acquired on the Agilent spectrometer using the Dbppste (DOSY) bipolar pulse pair stimulated echo pulse sequence. Typically, 32 gradient levels ranging from 6 to 55 G cm^{-1} and 16 transients were used. The diffusion time was 50 ms with a total diffusion-encoding gradient duration of 3 ms. Spectra were recorded in $CDCl_3$ or dry CD_3CN and referenced internally to residual solvent (^1H) or externally to $CFCl_3$ (^{19}F) or $BF_3{\cdot}OEt_2$ (^{11}B). NMR resonances were unambiguously assigned based on additional 2D NMR experiments (^1H-^1H COSY). Figure 10 shows the labelling scheme for NMR assignments used in the following experimental protocols. Mass spectra were obtained by positive ion electrospray ionisation using a Thermo Fisher Orbitrap mass spectrometer. Elemental analysis for carbon, hydrogen, and nitrogen was performed using a PerkinElmer 240 Elemental Analyser.

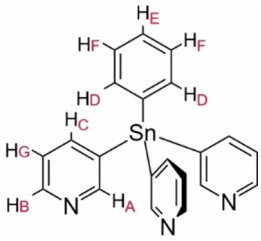

Figure 10. Labelling scheme for NMR assignments of ligand **1**.

X-ray crystallographic data were collected using a D8-QUEST PHOTON-100 diffractometer equipped with an Incoatec IμS Cu microsource ($Cu_{K\alpha}$, $\lambda = 1.5418$ Å). The temperature was held at 180(2) K using an Oxford Cryosystems N_2 cryostat. Data integration and reduction were undertaken with SAINT in the APEX3 software suite. Multi-scan corrections were applied using SADABS. Structures were solved using SHELXT[26] and refined using SHELXL.[27] Data for $[CoCl_2(\mathbf{1})(MeOH)]$ were collected at Beamline I19 of Diamond Light Source employing silicon double crystal monochromated synchrotron radiation (0.6889 Å) with ω and φ scans at 100(2) K.[28] Data integration and reduction were undertaken with Xia2.[29] Multi-scan empirical absorption corrections were applied to the data using the AIMLESS[30] tool in the CCP4 suite.[31] The structure was solved using SHELXT then refined with SHELXL.

Synthesis of SnPh(3-Py)$_3$ (1): 3-Pyridylmagnesium chloride lithium chloride complex was prepared in situ using a previously reported procedure.[24] 3-Bromopyridine (0.96 mL, 10.0 mmol) was added in one portion to a stirred solution of 1.3 M isopropylmagnesium chloride lithium chloride complex in THF (8.08 mL, 10.5 mmol) at -15 °C under a nitrogen atmosphere. The resulting brown mixture

was stirred for 15 min at −10 °C. Phenyltin trichloride (0.55 mL, 3.3 mmol) was added dropwise to the reaction mixture, which was then allowed to warm to room temperature and stirred overnight. The resulting white suspension was treated with water (20 mL), and the organic phase extracted with dichloromethane (3×15 mL). The extract was washed with brine (15 mL), dried over anhydrous magnesium sulfate, then filtered through Celite. The solvent was removed by evaporation under reduced pressure to give a pale yellow-orange solid, which was purified by recrystallisation (dichloromethane/hexane) and washed with acetone to yield phenyltris(3-pyridyl)stannane (1) as colourless needle-like crystals (0.52 g, 1.2 mmol, 36%). The reaction was found to work best on this scale. Single crystals suitable for X-ray diffraction were obtained by vapour diffusion recrystallisation from dichloromethane/pentane. Elemental analysis (%) calcd for $C_{21}H_{18}N_3Sn$: C 58.65, H 3.98, N 9.77, found: C 58.50, H 3.93, N 9.68. ^{1}H NMR (25 °C, $CDCl_3$, 400 MHz): δ = 8.74 (s, 3H, H_A), 8.67 (dd, J_{HH} = 2 Hz, 5 Hz, 3H, H_B), 7.86 (d, J_{HH} = 8 Hz, 3H, H_C), 7.56 (m, 2H, H_D), 7.46 (m, 3H, $H_{E/F}$), 7.35 ppm (dd, J_{HH} = 5 Hz, 8 Hz, 3H, H_G). ^{1}H NMR (25 °C, CD_3CN, 400 MHz): δ = 8.70 (dd, J_{HH} = 1 Hz, 3H, H_A), 8.61 (dd, J_{HH} = 2 Hz, 5 Hz, 3H, H_B), 7.93 (ddd, J_{HH} = 2 Hz, 7 Hz, J_{HSn} = 48 Hz, 3H, H_C), 7.62 (m, 2H, H_D), 7.47 (m, 3H, $H_{E/F}$), 7.38 ppm (ddd, J_{HH} = 1 Hz, 5 Hz, 7 Hz, 3H, H_G). HRMS-ESI (*m/z*) calcd for $C_{21}H_{18}N_3{}^{120}Sn_1$ ($M+H^+$): 432.0521, found: 432.0518.

Synthesis of $[Cu_2I_2(1)_2]_n$: A solution of copper(I) iodide (22 mg, 0.12 mmol) in dry acetonitrile (2 mL) was prepared in a narrow Schlenk flask under a nitrogen atmosphere. A solution of phenyltris(3-pyridyl)stannane (**1**) (50 mg, 0.12 mmol) in dry acetonitrile (12 mL) was layered carefully on top of the copper iodide solution. The two layers were left to diffuse slowly at room temperature over 72 h, resulting in yellow crystals that were isolated by filtration. The product $[Cu_2I_2(\mathbf{1})_2]_n$ was obtained as yellow crystals (49 mg, 0.079 mmol, 66%). Characterisation of the product by NMR spectroscopy and mass spectrometry was impeded by its insolubility in suitable solvents. Elemental analysis (%) calcd for $C_{42}H_{34}Cu_2I_2N_6Sn_2$: C 40.65, H 2.76, N 6.77, found: C 40.78, H 2.68, N 6.23.

Synthesis of $[Cu(1)(NCMe)]_4[PF_6]_4$: A Schlenk flask was charged with tetrakis(acetonitrile)copper(I) hexafluorophosphate (87 mg, 0.23 mmol) in a nitrogen filled glove box. The flask was transferred to a Schlenk line, and the solid dissolved in dry acetonitrile (4 mL) to give a colourless solution. To this, a solution of phenyltris(3-pyridyl)stannane (**1**) (100 mg, 0.23 mmol) in dry dichloromethane (12 mL) was added. The resulting yellow mixture was stirred at room temperature overnight, then filtered through Celite. Removal of the solvent in vacuo yielded $[Cu(\mathbf{1})(NCMe)]_4[PF_6]_4$ as a yellow solid (0.14 g, 0.21 mmol, 91%). Single crystals suitable for X-ray diffraction were obtained by vapour diffusion recrystallisation from acetonitrile/ether. Elemental analysis (%) calcd for $C_{92}H_{80}Cu_4F_{24}N_{16}P_4Sn_4$: C 40.65, H 2.97, N 8.24, found: C 41.15, H 3.29, N 8.12. ^{1}H NMR (−30 °C, CD_3CN, 500 MHz): δ = 8.33 (d, J_{HH} = 4 Hz, 3H, H_B), 7.91 (d, J_{HH} = 7 Hz, 3H, H_C), 7.68 (s, 3H, H_A), 7.49 (d, J_{HH} = 6 Hz, 2H, H_D), 7.42 (b), 7.41 ppm (b). ^{1}H NMR (70 °C, CD_3CN, 500 MHz): δ = 8.70 (s, 3H, H_A), 8.31 (d, J_{HH} = 5 Hz, 3H, H_B), 7.97 (d, J_{HH} = 7 Hz, 3H, H_C), 7.63 (m, 2H, H_D), 7.49 (m, 3H, $H_{E/F}$), 7.42 ppm (dd, J_{HH} = 5 Hz, 7 Hz, 3H, H_G). ^{19}F NMR (−30 °C, CD_3CN, 470.6 MHz): δ = −70.99 (d, J_{FP} = 707 Hz, PF_6), −71.05 (d, J_{FP} = 707 Hz, PF_6), −71.12 (d, J_{FP} = 707 Hz, PF_6), −72.79 ppm (d, J_{FP} = 707 Hz, PF_6). ^{19}F NMR (70 °C, CD_3CN, 470.6 MHz): δ = −73.50 ppm (d, J_{FP} = 706 Hz, PF_6). HRMS-ESI (*m/z*) calcd for $C_{23}H_{20}CuN_4{}^{120}Sn_1$ ($[Cu(\mathbf{1})(NCMe)]^+$): 535.0003, found: 535.0010.

Synthesis of $\{[Ag(1)(NCMe)]PF_6{\cdot}OEt_2\}_n$: A Schlenk flask was charged with silver(I) hexafluorophosphate (59 mg, 0.23 mmol) in a nitrogen filled glove box. The flask was transferred to a Schlenk line, and the solid dissolved in dry acetonitrile (4 mL) to give a colourless solution. To this, a solution of phenyltris(3-pyridyl)stannane (**1**) (100 mg, 0.23 mmol) in dry dichloromethane (12 mL) was added. The reaction mixture was stirred at room temperature overnight, then filtered through Celite. The solvent was removed in vacuo to give a colourless solid. Recrystallisation from acetonitrile/ether by liquid-diffusion yielded the product $\{[Ag(\mathbf{1})(NCMe)]PF_6{\cdot}Et_2O\}_n$ as colourless crystals (76 mg, 0.095 mmol, 41%). Elemental analysis (%) calcd for $C_{23}H_{20}AgF_6N_4PSn$: C 38.16, H 2.78, N 7.74, found: C 38.34, H 3.06, N 8.02. ^{1}H NMR (25 °C, CD_3CN, 400 MHz): δ = 8.67 (s, 3H, H_A), 8.60 (dd, J_{HH} = 1 Hz, 5 Hz, 3H, H_B), 8.02 (ddd, J_{HH} = 1 Hz, 7 Hz, 3H, H_C), 7.61 (m, 2H, H_D), 7.47 ppm (m, 6H, $H_{E/F/G}$). ^{19}F NMR (25 °C, CD_3CN, 376.5 MHz): δ = −73.20 ppm (d, J_{FP} = 707 Hz, PF_6). HRMS-ESI (*m/z*) calcd for $C_{23}H_{20}AgN_4{}^{120}Sn_1$ ($[Ag(\mathbf{1})(NCMe)]^+$): 578.9761, found: 578.9764.

Synthesis of $[CoCl_2(1)(MeOH)]_n$: A Schlenk flask was charged with cobalt(II) chloride (18 mg, 0.14 mmol) in a nitrogen filled glove box. The solid was dissolved in methanol in air (3 mL). To this, a solution of phenyltris(3-pyridyl)stannane (**1**) (60 mg, 0.14 mmol) in methanol (3 mL) was added. The resulting pink solution was stirred at room temperature overnight. Slow evaporation of the solvent afforded a blue solid product. Recrystallisation by vapour diffusion from methanol/ether yielded $[CoCl_2(\mathbf{1})(MeOH)]_n$ as pink crystals (39 mg, 0.066 mmol, 47%). Characterisation of the product by NMR spectroscopy was impeded by its paramagnetism. Satisfactory elemental analysis could not be achieved due to partial loss of MeOH from the complex upon drying. The complex was only characterised by single-crystal X-ray analysis.

Synthesis of $[Co_5(1)_6(H_2O)_6(NCMe)_6][BF_4]_{10}$: A solution of phenyltris(3-pyridyl)stannane (**1**) (20 mg, 0.047 mmol) in dichloromethane (3 mL) was prepared in a narrow Schlenk flask. A solution of cobalt(II) tetrafluoroborate hexahydrate (16 mg, 0.047 mmol) in acetonitrile (1 mL) was layered carefully on top of the solution of **1**. The two layers were left to diffuse slowly at −30 °C, resulting in the growth of the product $[Co_5(\mathbf{1})_6(H_2O)_6(NCMe)_6][BF_4]_{10}$ as pink needle-like crystals (16.9 mg, 0.027 mmol, 58%). Characterisation of the product by ^{1}H NMR spectroscopy was impeded by its paramagnetism. Satisfactory elemental analysis could not be achieved due to partial loss of coordinated solvent from the complex upon drying. ^{11}B NMR (25 °C, CD_3CN, 128.4 MHz): δ = 32.86 (s, *endo*-BF_4), 0.09 ppm (s, *exo*-BF_4). ^{19}F NMR (25 °C, CD_3CN, 376.5 MHz): δ = −112.75 (s, *endo*-BF_4), −145.59 ppm (s, *exo*-BF_4).

Acknowledgements

We thank the Leverhulme Trust (DSW, RGR, postdoctoral research grant for A.L.C.), the Spanish MINECO-AEI and the EU (ESF) for a Ramon y Cajal contract (RG-R, RYC-2015-19035), the Spanish MCIU for funding (PGC2018-096880-A-I00, MCIU/AEI/FEDER, UE) and the Cambridge Trust (Vice Chancellor Scholarship for A.J.P.). We also thank Diamond Light Source (UK, MT15768) for synchrotron X-ray data collection on $[CoCl_2(\mathbf{1})(MeOH)]_n$.

Conflict of interest

The authors declare no conflict of interest.

Keywords: encapsulation · coordination polymers · supramolecular chemistry · tin · tris(pyridyl) ligands

[1] N. N. Adarsh, P. Dastidar, *Chem. Soc. Rev.* **2012**, *41*, 3039 – 3060.
[2] M. D. Wise, J. J. Holstein, P. Pattison, C. Besnard, E. Solari, R. Scopelliti, G. Bricogne, K. Severin, *Chem. Sci.* **2015**, *6*, 1004 – 1010.
[3] S. M. Jansze, G. Cecot, M. D. Wise, K. O. Zhurov, T. K. Ronson, A. M. Castilla, A. Finelli, P. Pattison, E. Solari, R. Scopelliti, G. E. Zelinskii, A. V. Vologzhanina, Y. Z. Voloshin, J. R. Nitschke, K. Severin, *J. Am. Chem. Soc.* **2016**, *138*, 2046 – 2054.
[4] Y.-J. Hou, K. Wu, Z.-W. Wei, K. Li, Y.-L. Lu, C.-Y. Zhu, J.-S. Wang, M. Pan, J.-J. Jiang, G.-Q. Li, C.-Y. Su, *J. Am. Chem. Soc.* **2018**, *140*, 18183 – 18191.
[5] R. Saha, D. Samanta, A. J. Bhattacharyya, P. S. Mukherjee, *Chem. Eur. J.* **2017**, *23*, 8980 – 8986.
[6] M. Hardy, N. Struch, F. Topić, G. Schnakenburg, K. Rissanen, A. Lützen, *Inorg. Chem.* **2018**, *57*, 3507 – 3515.
[7] Y. Uchida, K. Matsuoka, R. Kajita, *Heteroat. Chem.* **1997**, *8*, 439 – 449.
[8] J. Y. Ryu, E. H. Wi, M. Pait, S. Lee, P. J. Stang, J. Lee, *Inorg. Chem.* **2017**, *56*, 5471 – 5477.
[9] J. Y. Ryu, Y. J. Park, H.-R. Park, M. L. Saha, P. J. Stang, J. Lee, *J. Am. Chem. Soc.* **2015**, *137*, 13018 – 13023.
[10] S. Chen, K. Li, F. Zhao, L. Zhang, M. Pan, Y.-Z. Fan, J. Guo, J. Shi, C.-Y. Su, *Nat. Commun.* **2016**, *7*, 13169.
[11] J. Guo, Y.-W. Xu, K. Li, L.-M. Xiao, S. Chen, K. Wu, X.-D. Chen, Y.-Z. Fan, J.-M. Liu, C.-Y. Su, *Angew. Chem. Int. Ed.* **2017**, *56*, 3852 – 3856; *Angew. Chem.* **2017**, *129*, 3910 – 3914.
[12] a) R. García-Rodríguez, S. Hanf, A. D. Bond, D. S. Wright, *Chem. Commun.* **2017**, *53*, 1225 – 1228; b) A. García-Romero, A. J. Plajer, L. Álvarez-Miguel, A. D. Bond, D. S. Wright, R. García-Rodríguez, *Chem. Eur. J.* **2018**, *24*, 17019 – 17026.
[13] S. Hanf, R. García-Rodríguez, A. D. Bond, E. Hey-Hawkins, D. S. Wright, *Dalton Trans.* **2016**, *45*, 276 – 283.
[14] A. J. Plajer, A. L. Colebatch, M. Enders, Á. García-Romero, A. D. Bond, R. García-Rodríguez, D. S. Wright, *Dalton Trans.* **2018**, *47*, 7036 – 7043.
[15] M. A. Beswick, C. J. Belle, M. K. Davies, M. A. Halcrow, P. R. Raithby, A. Steiner, D. S. Wright, *Chem. Commun.* **1996**, 2619 – 2620.
[16] A. J. Plajer, A. L. Colebatch, F. J. Rizzuto, P. Pröhm, A. D. Bond, R. García-Rodríguez, D. S. Wright, *Angew. Chem. Int. Ed.* **2018**, *57*, 6648 – 6652; *Angew. Chem.* **2018**, *130*, 6758 – 6762.
[17] V. Bocokić, A. Kalkan, M. Lutz, A. L. Spek, D. T. Gryko, J. N. H. Reek, *Nat. Commun.* **2013**, *4*, 1 – 9.
[18] X. Wang, S. S. Nurttila, W. I. Dzik, R. Becker, J. Rodgers, J. N. H. Reek, *Chem. Eur. J.* **2017**, *23*, 14769 – 14777.
[19] M. S. Deshmukh, A. Yadav, R. Pant, R. Boomishankar, *Inorg. Chem.* **2015**, *54*, 1337 – 1345.
[20] M. S. Deshmukh, V. S. Mane, A. S. Kumbhar, R. Boomishankar, *Inorg. Chem.* **2017**, *56*, 13286 – 13292.
[21] A. M. Kluwer, I. Ahmad, J. N. H. Reek, *Tetrahedron Lett.* **2007**, *48*, 2999 – 3001.
[22] A. Krasovskiy, P. Knochel, *Angew. Chem. Int. Ed.* **2004**, *43*, 3333 – 3336; *Angew. Chem.* **2004**, *116*, 3396 – 3399.
[23] M. Mantina, A. C. Chamberlin, R. Valero, C. J. Cramer, D. G. Truhlar, *J. Phys. Chem. A* **2009**, *113*, 5806 – 5812.
[24] J. K. Clegg, L. F. Lindoy in *Anion Coordination Chemistry* (Eds.: K. Bowman-James, A. Bianchi, E. García-España), Wiley-VCH, Weinheim, **2011**.
[25] R. Custelcean, *Chem. Soc. Rev.* **2010**, *39*, 3675 – 3685.
[26] G. M. Sheldrick, *Acta Crystallogr. Sect. A* **2015**, *71*, 3 – 8.
[27] G. M. Sheldrick, *Acta Crystallogr. Sect. C* **2015**, *71*, 3 – 8.
[28] D. R. Allan, H. Nowell, S. A. Barnett, M. R. Warren, A. Wilcox, J. Christensen, L. K. Saunders, A. Peach, M. T. Hooper, L. Zaja, S. Patel, L. Cahill, R. Marshall, S. Trimnell, A. J. Foster, T. Bates, S. Lay, M. A. Williams, P. V. Hathaway, G. Winter, M. Gerstel, R. W. Wooley, *Crystals* **2017**, *7*, 336.
[29] G. Winter, *J. Appl. Crystallogr.* **2010**, *43*, 186 – 190.
[30] P. R. Evans, G. N. Murshudov, *Acta Crystallogr. Sect. D* **2013**, *69*, 1204 – 1214.
[31] M. D. Winn, C. C. Ballard, K. D. Cowtan, E. J. Dodson, P. Emsley, P. R. Evans, R. M. Keegan, E. B. Krissinel, A. G. W. Leslie, A. McCoy, S. J. McNicholas, G. N. Murshudov, N. S. Pannu, E. A. Potterton, H. R. Powell, R. J. Read, A. Vagin, K. S. Wilson, *Acta Crystallogr. Sect. D* **2011**, *67*, 235 – 242.

Manuscript received: July 31, 2019
Accepted manuscript online: August 30, 2019
Version of record online: October 9, 2019